Ocean Systems Engineering, *Vol. 7, No. 4 (2017) 399-412*
DOI: https:// doi.org/10.12989/ose.2017.7.4.399

A more efficient numerical evaluation of the green function in finite water depth

Zhitian Xie*, Yujie Liu and Jeffrey Falzarano

Department of Ocean Engineering, Texas A&M University, College Station, Texas, USA 77840

(Received June 2, 2017, Revised September 11, 2017, Accepted September 19, 2017)

Abstract. The Gauss-Legendre integral method is applied to numerically evaluate the Green function and its derivatives in finite water depth. In this method, the singular point of the function in the traditional integral equation can be avoided. Moreover, based on the improved Gauss-Laguerre integral method proposed in the previous research, a new methodology is developed through the Gauss-Legendre integral. Using this new methodology, the Green function with the field and source points near the water surface can be obtained, which is less mentioned in the previous research. The accuracy and efficiency of this new method is investigated. The numerical results using a Gauss-Legendre integral method show good agreements with other numerical results of direct calculations and series form in the far field. Furthermore, the cases with the field and source points near the water surface are also considered. Considering the computational efficiency, the method using the Gauss-Legendre integral proposed in this paper could obtain the accurate numerical results of the Green function and its derivatives in finite water depth and can be adopted in the near field.

Keywords: green function; finite water depth; numerical evaluation; Gauss-Legendre integral

1. Introduction

The hydrodynamic motion and load response of offshore structures in finite water depth present different characteristics compared with those in deep water. Only when the precise solution of the Green function and its partial derivatives in finite water depth are obtained, is it possible to acquire an accurate motion response prediction of floating structures in finite water depth. Therefore, an accurate and efficient numerical evaluation of the Green function and its partial derivatives for a pulsating source in finite water depth is one of the most important aspects in the theory of potential flow applied to marine hydrodynamics. The development of fast computers makes it possible to conduct numerical calculations for three dimensional flows, which has also caused a search for expressions of the Green function in finite water depth with efficient numerical evaluation.

Noblesse (1982, 1983, 1986) conducted the study concerned with the Green function and the general identity for the velocity potential of the potential flow theory about a body in regular waves in deep water. Wu (2017) expressed the Green function of the theory of diffraction radiation and its gradient in deep water as the sum of three components corresponding to the fundamental

*Corresponding author, Ph.D. Student, E-mail: xiezhitian@tamu.edu

http://www.techno-press.org/?journal=ose&subpage=7 ISSN: 2093-6702 (Print), 2093-677X (Online)

free-space singularity, a non-oscillatory local flow and waves, using simple and global approximations involving elementary continuous functions within the entire flow region. The expression of the Green function in finite water depth mainly has two forms. One is the series expression proposed by John (1950), the other one is the integral form proposed by Wehausen and Laitone (1960). The series form presents a high computational efficiency. However, it is difficult to converge in the near field due to the existence of a singularity at $R = 0$, on one hand. On the other hand, the integral form presents a high accuracy but low computational efficiency in the far field. Therefore, to calculate the Green function and its partial derivatives in finite water depth, an algorithm has been proposed to utilize the integral form for the near field and the series form for the far field. For the integral form, due to the singularity in the Cauchy principal value integral and the oscillatory behavior of Bessel function, it is also one of the most challenging tasks to accurately evaluate the Green function in finite water depth. Li (2001) has applied Gauss-Laguerre integration to numerically evaluate the Green function and its partial derivatives in finite water depth, which transfers the integral form to the summation form. Some results have been shown in this scenario to investigate the effect of forward speed on the wave loads in restricted water depth by Guha (2016). In Li's method, the results from the Gauss-Laguerre integration is not stable for the far field and is slow to converge. Moreover, the result of the Green function with the field and source points near the water surface is not mentioned. Liu (2008) and Yang (2014) have developed an improved Gauss-Laguerre method, using a reduced fraction to separate the parts that can be calculated by the Green function in infinite water depth, in order to decrease the integral variable's order of the rest of the integral functions. The numerical results of this improved Gauss-Laguerre method may lose precision in some cases. Wu (2017).

Therefore, this study is concerned with constructing an alternative integral method for the Green function from the theory of linearized potential flow due to a source of pulsating strength in finite water depth. Both the precision and computational efficiency of the Gauss-Legendre integral method proposed in this paper are considered. Since the asymptotic behavior of the Green function in finite water depth is worth being investigated, especially in solving the wave resistance calculations by Yu (2017), 3-D energy balance in a wave field interacting with the OWC system by Wang (2017), and the irregular frequency removal problem and drift force calculation discussed by Liu (2016, 2017). This work will present a meaningful reference with details to numerically evaluate the Green function in finite water depth to further solve the ship moving problem.

2. Introduction of the Gauss-Laguerre integral method

The Green function in finite water depth can be expressed in terms of integral as follows (Wehausen and Laitone 1960)

$$G = \frac{1}{r} + \frac{1}{r^*} + G_{IR2} \tag{1}$$

Where

$$G_{IR2} \cdot h = 2PV \int_0^\infty \frac{e^{-x} \cdot (x + Kh) \cdot \cosh(x(r_2+1)) \cdot \cosh(x(r_3+1)) \cdot J_0(xr_1)}{x \cdot \sinh(x) - Kh \cdot \cosh(x)} dx \tag{2}$$

$$K = \frac{\omega^2}{g} = k \cdot \tanh(kh)$$

$$r = [(x-\xi)^2 + (y-\eta)^2 + (z-\zeta)^2]^{\frac{1}{2}}$$

$$r^* = [(x-\xi)^2 + (y-\eta)^2 + (z+\zeta+2h)^2]^{\frac{1}{2}}$$

$$R = [(x-\xi)^2 + (y-\eta)^2]^{\frac{1}{2}}$$

$$r_1 = \frac{R}{h} \qquad r_2 = \frac{\zeta}{h} \qquad r_3 = \frac{z}{h}$$

$p = p(x,y,z)$ is the field point; $q = q(\xi,\eta,\zeta)$ is the source point; h is the water depth; k is the wave number. PV is the Cauchy principal value of the integral with a singularity $x_0 = k{\cdot}h$. J_0 indicates the first kind Bessel function with zero order.

The partial derivatives of the Green function in finite water depth can be so thus expressed as follows

$$\frac{\partial G_{IR2}}{\partial R}.h^2 = -2PV\int_0^\infty \frac{e^{-x}\cdot x.(x+Kh)\cdot\cosh(x(r_2+1))\cdot\cosh(x(r_3+1))\cdot J_1(xr_1)}{x\cdot\sinh(x)-Kh\cdot\cosh(x)}dx \tag{3}$$

$$\frac{\partial G_{IR2}}{\partial z}.h^2 = 2PV\int_0^\infty \frac{e^{-x}\cdot x.(x+Kh)\cdot\cosh(x(r_2+1))\cdot\sinh(x(r_3+1))\cdot J_0(xr_1)}{x\cdot\sinh(x)-Kh\cdot\cosh(x)}dx \tag{4}$$

Considering the computational efficiency, a strategy is proposed that the integral form can be applied when $R/h \le 0.5$ and the series form can be applied for $R/h > 0.5$ (Newman, 1985).

Li (2001) separated the Green function in finite water depth into two parts as follows

$$G_{IR2}\cdot h = 2PV\int_0^\infty e^{-x}\cdot\Big[\frac{(x+Kh)\cdot\cosh(x(r_2+1))\cdot\cosh(x(r_3+1))\cdot J_0(xr_1)}{x\cdot\sinh(x)-Kh\cdot\cosh(x)} - \frac{(kh+Kh)\cdot\cosh(kh(r_2+1))\cdot\cosh(kh(r_3+1))\cdot J_0(r_1\cdot kh)}{(x-kh)\cdot(\sinh(kh)+kh\cdot\cosh(kh)-Kh\cdot\sinh(kh))}\Big]dx - 2e^{-kh}Ei(kh)\frac{(kh+Kh)\cdot\cosh(kh(r_2+1))\cdot\cosh(kh(r_3+1))\cdot J_0(r_1\cdot kh)}{\sinh(kh)+kh\cdot\cosh(kh)-Kh\cdot\sinh(kh)} \tag{5}$$

Where

$$PV\int_0^\infty \frac{1}{(x-a)}\cdot e^{-x}dx = -e^{-a}\cdot E_i(a) \tag{6}$$

Therefore, the first part is the Cauchy principal value which can be approximated by the Gauss-Laguerre integral and the value of the second part can be calculated through the exponential integral. The Gauss-Laguerre quadrature can be expressed as follows

$$\int_0^\infty e^{-x}f(x)dx \approx \sum_{j=1}^{N}\omega_j f(x_j) \tag{7}$$

Where: x_j is the j^{th} zero of the Laguerre polynomial $L_n(x)$ and ω_j is the weight.

The numerical results from this method are slow to converge and may lose precision at high wave frequency. Liu (2008) separated the function in the Cauchy principal integral to isolate the exponential terms that cause the numerical error in the traditional Gauss-Laguerre integral method.

In this scenario, the exponential term containing $e^{x(1+r_2+r_3)}$ to be integrated was particularly treated by using the Green function in infinite water depth. After that, Yang (2014) developed an improved Gauss-Laguerre integral method by handling the other exponential terms to obtain the accurate values of the Green function and its derivatives in finite water depth. This improved method could obtain the numerical value of the Green function correctly, but may lose precision in the far field and in some cases with high wave frequency.

3. Gauss-Legendre integral method

From the previous research of Liu (2008) and Yang (2014), the Green function in finite water depth can be transformed as follows

$$G_{IR2}\cdot h = 2PV\int_0^\infty \frac{e^{-x}\cdot(x+Kh)\cdot\cosh(x(r_2+1))\cdot\cosh(x(r_3+1))\cdot J_0(xr_1)}{x\cdot\sinh(x)-Kh\cdot\cosh(x)}dx$$
$$= PV\int_0^\infty \frac{(x+Kh)\cdot(e^{xr_2}+e^{x(-2-r_2)})\cdot(e^{xr_3}+e^{x(-2-r_3)})\cdot J_0(xr_1)}{(x-Kh)-e^{-2x}(x+Kh)}dx$$
$$= PV\int_0^\infty [1+\frac{2Kh+e^{-2x}(x+Kh)}{(x\cdot\tanh(x)-Kh)\cdot(1+e^{-2x})}]\cdot[e^{x(r_2+r_3)}+e^{x(-2-r_3+r_2)}+e^{x(-2-r_2+r_3)}+ e^{x(-4-r_2-r_3)}]\cdot J_0(xr_1)dx \quad (8)$$

Considering the Bessel functions (Newman 1984) and their integrals (Abramowitz 1964)

$$\int_0^\infty e^{-ax}J_0(bx)dx=\frac{1}{(a^2+b^2)^{0.5}}\ ,\ \int_0^\infty xe^{-ax}J_0(bx)dx=\frac{a}{(a^2+b^2)^{1.5}}$$
$$\int_0^\infty e^{-ax}J_1(bx)dx=(1-\frac{a}{(a^2+b^2)^{0.5}})\frac{1}{b}\ ,\ \int_0^\infty xe^{-ax}J_1(bx)dx=\frac{b}{(a^2+b^2)^{1.5}} \quad (9)$$

The Green function and its partial derivatives can be expressed as follows

$$G_{IR2}\cdot h = \frac{1}{(r_1^2+(r_2+r_3)^2)^{0.5}}+\frac{1}{(r_1^2+(2+r_3-r_2)^2)^{0.5}}+\frac{1}{(r_1^2+(2+r_2-r_3)^2)^{0.5}} +\frac{1}{(r_1^2+(4+r_2+r_3)^2)^{0.5}}+ PV\int_0^\infty \frac{2Kh+e^{-2x}(x+Kh)}{(x\cdot\tanh(x)-Kh)\cdot(1+e^{-2x})} \cdot[e^{x(r_2+r_3)}+e^{x(-2-r_3+r_2)}+e^{x(-2-r_2+r_3)}+ e^{x(-4-r_2-r_3)}]\cdot J_0(xr_1)dx \quad (10)$$

$$-\frac{\partial G_{IR2}}{\partial R}\cdot h^2 = \frac{r_1}{(r_1^2+(r_2+r_3)^2)^{1.5}}+\frac{r_1}{(r_1^2+(2+r_3-r_2)^2)^{1.5}}+\frac{r_1}{(r_1^2+(2+r_2-r_3)^2)^{1.5}} + \frac{r_1}{(r_1^2+(4+r_2+r_3)^2)^{1.5}} + PV\int_0^\infty \frac{2Kh+e^{-2x}(x+Kh)}{(x\cdot\tanh(x)-Kh)\cdot(1+e^{-2x})}\cdot[e^{x(r_2+r_3)} + e^{x(-2-r_3+r_2)}+e^{x(-2-r_2+r_3)}+e^{x(-4-r_2-r_3)}] \cdot x\cdot J_1(xr_1)dx \quad (11)$$

$$
\begin{aligned}
\frac{\partial G_{IR2}}{\partial z}\cdot h^2 = & \frac{-r_2-r_3}{(r_1^2+(r_2+r_3)^2)^{1.5}} - \frac{-r_2+r_3+2}{(r_1^2+(2+r_3-r_2)^2)^{1.5}} + \frac{-r_3+r_2+2}{(r_1^2+(2+r_2-r_3)^2)^{1.5}} \\
& - \frac{4+r_2+r_3}{(r_1^2+(4+r_2+r_3)^2)^{1.5}} \\
& + PV\int_0^{\infty} \frac{2Kh+e^{-2x}(x+Kh)}{(x\cdot\tanh(x)-Kh)\cdot(1+e^{-2x})}\cdot [e^{x(r_2+r_3)} \\
& - e^{x(-2-r_3+r_2)} + e^{x(-2-r_2+r_3)} - e^{x(-4-r_2-r_3)}] \\
& \cdot x\cdot J_0(xr_1)dx
\end{aligned} \quad (12)
$$

For a Cauchy principal integral $PV\int_0^{\infty}\left(\frac{f(x)}{g(x)}-\frac{f(a)}{(x-a)\cdot g'(a)}\right)dx$, the point $x=a$ is the unique singularity of $\frac{f(x)}{g(x)}-\frac{f(a)}{(x-a)\cdot g'(a)}$, whose limitation at this point is $\frac{2f'(a)g'(a)-g''(a)f(a)}{2(g'(a))^2}$ through l'Hôpital's Rule. Therefore, the integral with the integration interval from 0 to infinity can be divided into two integrals with the finite integration intervals

$$\int_0^{\infty}F(x)dx=\int_0^{a}F(x)dx+\int_0^{\frac{1}{a}}F(1/x)\cdot x^{-2}dx \quad (13)$$

The Gauss-Legendre integration formula is applied to approximate the integral with finite integration interval as follows

$$
\begin{aligned}
\int_a^{b} f(y)dy \approx \frac{b-a}{2}\sum_{j=1}^{N}\omega_j f(y_j) \\
y_j=\left(\frac{b-a}{2}\right)x_j+\frac{b+a}{2}
\end{aligned} \quad (14)
$$

Where: x_j is the j^{th} zero of the Legendre polynomial $P_n(x)$, $P_n(1)=1$. $\omega_j=2/\left(1-x_j^2\right)[P_n'(x_j)]^2$.

According to the definition, the term r_2+r_3 is from -2 to 0, while $-2\pm r_3-(\pm r_2)$ and $-2-r_3-r_2$ are from -3 to -1 and -4 to -2, respectively. When the field point and the source point are both close to the water surface, namely r_2+r_3 is from -0.2 to 0, the exponential term $e^{x(r_2+r_3)}$ converges much slower than the other three exponential terms. In this scenario, the integral with $e^{x(r_2+r_3)}$ is handled specially through the Green function in infinite water depth to leave the Bessel function in the integral to help the whole function $\left(\frac{f(x)}{g(x)}-\frac{f(a)}{(x-a)\cdot g'(a)}\right)\cdot e^{x(r_2+r_3)}\cdot J_0(xr_1)$ converges faster. Therefore, less zero points of the Legendre polynomial are needed to evaluate the integral with certain accuracy, which contributes to a higher computational efficiency. The integral with $e^{x(-2-r_3+r_2)}+e^{x(-2-r_2+r_3)}+e^{x(-4-r_2-r_3)}$ is evaluated by substituting Bessel function into the function $f(x)$, since the function $\left(\frac{f(x)}{g(x)}-\frac{f(a)}{(x-a)\cdot g'(a)}\right)\cdot(e^{x(-2-r_3+r_2)}+e^{x(-2-r_2+r_3)}+e^{x(-4-r_2-r_3)})$ itself converges fast enough. Therefore, the expressions of the integral forms are as follows:

For the integral containing $e^{x(r_2+r_3)}$

$$PV\int_0^{\infty}\frac{f(x)}{g(x)}\cdot e^{x(r_2+r_3)}\cdot J_0(xr_1)dx = PV\int_0^{\infty}\left(\frac{f(x)}{g(x)}-\frac{f(a)}{(x-a)\cdot g'(a)}\right)\cdot\ e^{x(r_2+r_3)}\cdot J_0(xr_1)dx+\frac{f(a)}{g'(a)}\cdot$$

$$PV\int_0^\infty \frac{1}{(x-a)}\cdot e^{x(r_2+r_3)}\cdot J_0(xr_1)dx \tag{15}$$

Where

$$f(x) = 2Kh + e^{-2x}(x+Kh)$$
$$g(x) = (x\cdot\tanh(x) - Kh)\cdot(1+e^{-2x})$$

$PV\int_0^\infty \frac{1}{(x-a)}\cdot e^{xr}\cdot J_0(xr_1)dx$ can be evaluated from the Green function in infinite water depth (Wang, 1992).

For the integral containing $e^{x(-2-r_3+r_2)} + e^{x(-2-r_2+r_3)} + e^{x(-4-r_2-r_3)}$

$$V\int_0^\infty \frac{f(x)}{g(x)}\cdot(e^{x(-2-r_3+r_2)} + e^{x(-2-r_2+r_3)} + e^{x(-4-r_2-r_3)})dx$$
$$= PV\int_0^\infty\left(\frac{f(x)}{g(x)} - \frac{f(a)}{(x-a)\cdot g'(a)}\right)\cdot\ (e^{x(-2-r_3+r_2)} + e^{x(-2-r_2+r_3)}$$
$$+ e^{x(-4-r_2-r_3)})\,dx + \frac{f(a)}{g'(a)}\cdot PV\int_0^\infty \frac{1}{(x-a)}\cdot(e^{x(-2-r_3+r_2)} +$$
$$e^{x(-2-r_2+r_3)} + e^{x(-4-r_2-r_3)})dx \tag{16}$$

Where

$$PV\int_0^\infty \frac{1}{(x-a)}\cdot e^{-x}dx = -e^{-a}\cdot E_i(a)$$
$$f(x) = (2Kh + e^{-2x}(x+Kh))\cdot J_0(xr_1)$$
$$g(x) = (x\cdot\tanh(x) - Kh)\cdot(1+e^{-2x})$$

Similarly, the integral forms of the Green function's partial derivatives can be obtained.

$\frac{\partial G_{IR2}}{\partial R}\cdot h^2$:

For the integral containing $e^{x(r_2+r_3)}$

$$PV\int_0^\infty \frac{f(x)}{g(x)}\cdot e^{x(r_2+r_3)}\cdot x\cdot J_1(xr_1)dx = PV\int_0^\infty\left(\frac{f(x)}{g(x)} - \frac{f(a)}{(x-a)\cdot g'(a)}\right)\cdot e^{x(r_2+r_3)}\cdot\ x\cdot J_1(xr_1)dx +$$
$$\frac{f(a)}{g'(a)}\cdot PV\int_0^\infty \frac{x}{(x-a)}\cdot e^{x(r_2+r_3)}\cdot J_1(xr_1)dx \tag{17}$$

Where

$$f(x) = 2Kh + e^{-2x}(x+Kh)$$
$$g(x) = (x\cdot\tanh(x) - Kh)\cdot(1+e^{-2x})$$

For the integral containing $e^{x(-2-r_3+r_2)} + e^{x(-2-r_2+r_3)} + e^{x(-4-r_2-r_3)}$

$$V\int_0^\infty \frac{f(x)}{g(x)}\cdot(e^{x(-2-r_3+r_2)} + e^{x(-2-r_2+r_3)} + e^{x(-4-r_2-r_3)})dx$$
$$= PV\int_0^\infty\left(\frac{f(x)}{g(x)} - \frac{f(a)}{(x-a)\cdot g'(a)}\right)\cdot(e^{x(-2-r_3+r_2)} + e^{x(-2-r_2+r_3)} + e^{x(-4-r_2-r_3)})\,dx$$
$$+ \frac{f(a)}{g'(a)}\cdot PV\int_0^\infty \frac{1}{(x-a)}\cdot(e^{x(-2-r_3+r_2)} +$$

$$e^{x(-2-r_2+r_3)} + e^{x(-4-r_2-r_3)})dx \tag{18}$$

Where

$$f(x) = (2Kh + e^{-2x}(x + Kh)) \cdot x \cdot J_1(xr_1)$$
$$g(x) = (x \cdot \tanh(x) - Kh) \cdot (1 + e^{-2x})$$

$\frac{\partial G_{IR2}}{\partial z} \cdot h^2$

For the integral containing $e^{x(r_2+r_3)}$

$$PV\int_0^\infty \frac{f(x)}{g(x)} \cdot e^{x(r_2+r_3)} \cdot x \cdot J_0(xr_1)dx = PV\int_0^\infty \left(\frac{f(x)}{g(x)} - \frac{f(a)}{(x-a)\cdot g'(a)}\right) \cdot e^{x(r_2+r_3)} \cdot x \cdot J_0(xr_1)dx + \frac{f(a)}{g'(a)} \cdot PV\int_0^\infty \frac{x}{(x-a)} \cdot e^{x(r_2+r_3)} \cdot J_0(xr_1)dx \tag{19}$$

Where

$$f(x) = 2Kh + e^{-2x}(x + Kh)$$
$$g(x) = (x \cdot \tanh(x) - Kh) \cdot (1 + e^{-2x})$$

For the integral containing $e^{x(-2-r_3+r_2)} + e^{x(-2-r_2+r_3)} + e^{x(-4-r_2-r_3)}$

$$PV\int_0^\infty \frac{f(x)}{g(x)} \cdot (-e^{x(-2-r_3+r_2)} + e^{x(-2-r_2+r_3)} - e^{x(-4-r_2-r_3)})dx$$
$$= PV\int_0^\infty \left(\frac{f(x)}{g(x)} - \frac{f(a)}{(x-a)\cdot g'(a)}\right) \cdot (-e^{x(-2-r_3+r_2)} + e^{x(-2-r_2+r_3)} - e^{x(-4-r_2-r_3)})\,dx + \frac{f(a)}{g'(a)} \cdot PV\int_0^\infty \frac{1}{(x-a)} \cdot (-e^{x(-2-r_3+r_2)} +$$
$$e^{x(-2-r_2+r_3)} - e^{x(-4-r_2-r_3)})dx \tag{20}$$

Where

$$f(x) = (2Kh + e^{-2x}(x + Kh)) \cdot x \cdot J_0(xr_1)$$
$$g(x) = (x \cdot \tanh(x) - Kh) \cdot (1 + e^{-2x})$$

Therefore, the Green function and its partial derivatives in finite water depth can be expressed as the summation of the special functions (Ei and the Green function in infinite water depth) and integrals that can be evaluated through the Gauss-Legendre integral method.

4. Results and discussion

The Green function and its partial derivatives in finite water depth can be regarded as functions of kh, R/h, z/h and ζ/h. The values of the Green function and its partial derivatives through the Gauss-Legendre integral method are compared with those from direct integral calculation using Romberg's method and series form both in the near field and far field to verify the accuracy of the new method proposed in this paper. The numerical calculations with two different wave frequencies (kh = 0.46268 and 2.06534) are conducted. Moreover, the cases with the field and source points near the water surface are also considered as a comparison with the cases with the field point near the water bottom.

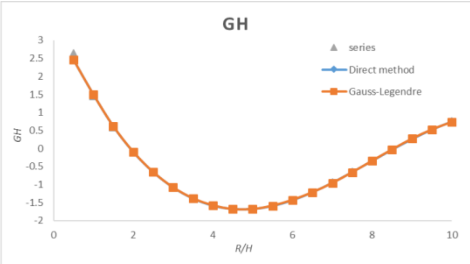

(a) Gh

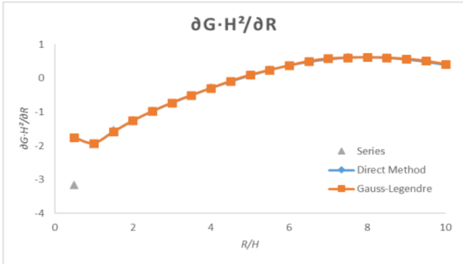

(b) $\frac{\partial G}{\partial R} \cdot h^2$

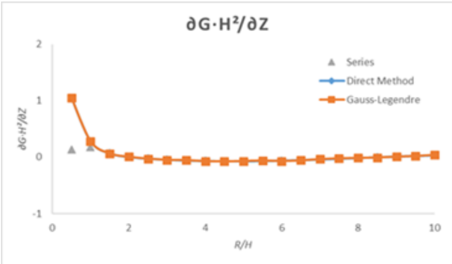

(c) $\frac{\partial G}{\partial z} \cdot h^2$

Fig. 1 The Green function and its derivatives (kh = 0.46268, $\zeta/h = 0$, z/h = -0.8 for (c), z/h = -1 for (a) and (b))

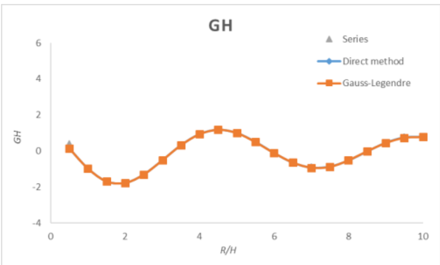

(a) Gh

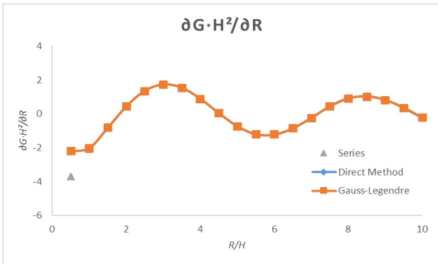

(b) $\frac{\partial G}{\partial R} \cdot h^2$

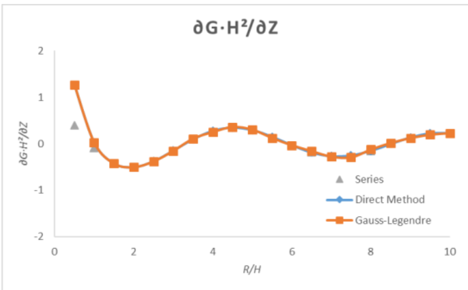

(c) $\frac{\partial G}{\partial z} \cdot h^2$

Fig. 2 The Green function and its derivatives (kh = 1.19968, $\zeta/h = 0$, z/h = -0.8 for (c), z/h = -1 for (a) and (b))

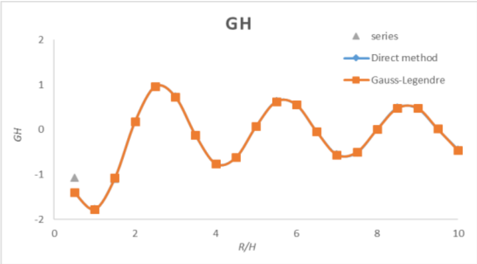

(a) Gh

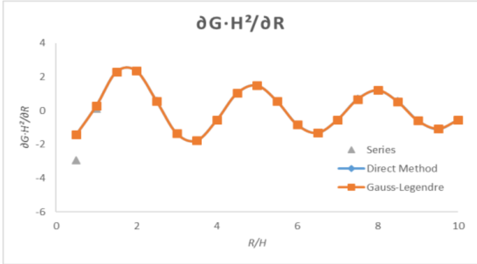

(b) $\frac{\partial G}{\partial R} \cdot h^2$

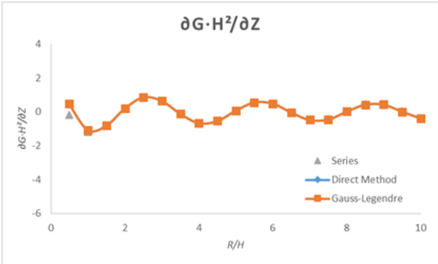

(c) $\frac{\partial G}{\partial z} \cdot h^2$

Fig. 3 The Green function and its derivatives (kh = 2.06534, $\zeta/h = 0$, z/h = -0.8 for (c), z/h = -1 for (a) and (b))

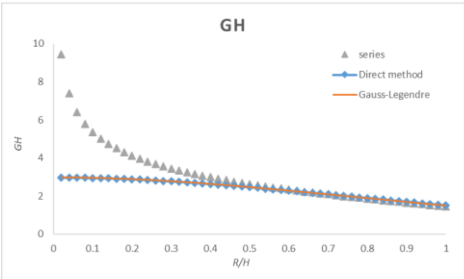

(a) Gh

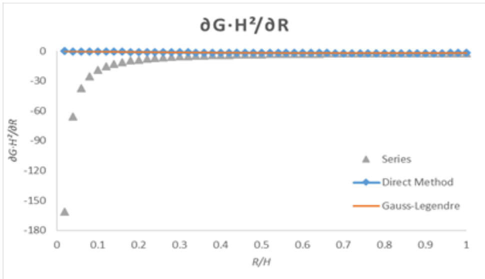

(b) $\frac{\partial G}{\partial R} \cdot h^2$

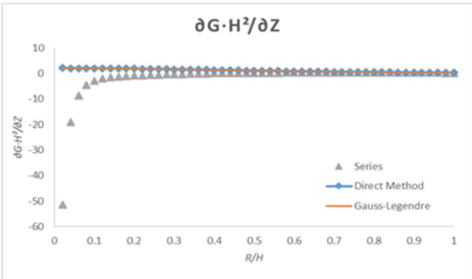

(c) $\frac{\partial G}{\partial z} \cdot h^2$

Fig. 4 The Green function and its derivatives (Zoom in for Fig.1)

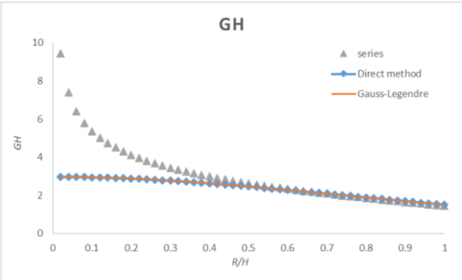

(a) Gh

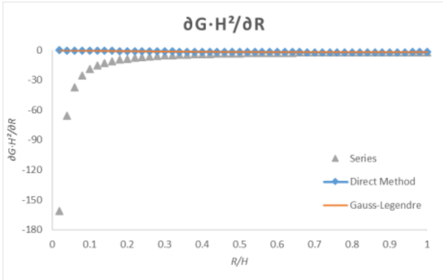

(b) $\frac{\partial G}{\partial R} \cdot h^2$

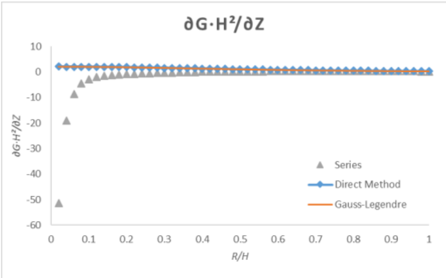

(c) $\frac{\partial G}{\partial z} \cdot h^2$

Fig. 5 The Green function and its derivatives (Zoom in for Fig. 2)

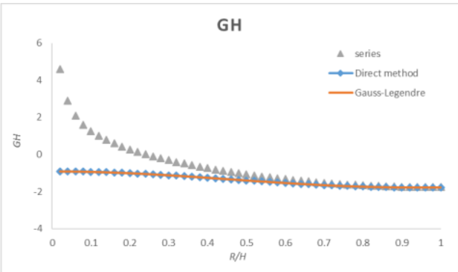

(a) Gh

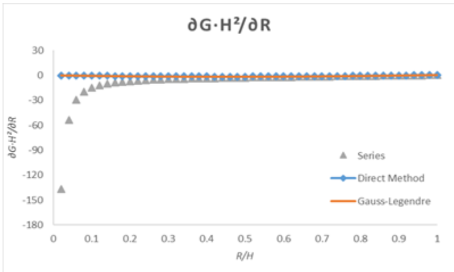

(b) $\frac{\partial G}{\partial R} \cdot h^2$

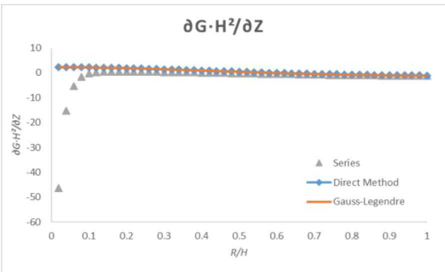

(c) $\frac{\partial G}{\partial z} \cdot h^2$

Fig. 6 The Green function and its derivatives (Zoom in for Fig. 3)

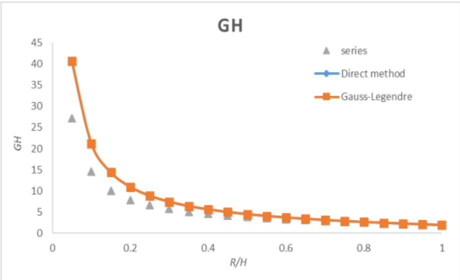

(a) Gh

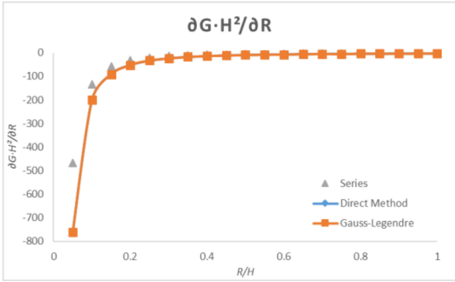

(b) $\frac{\partial G}{\partial R} \cdot h^2$

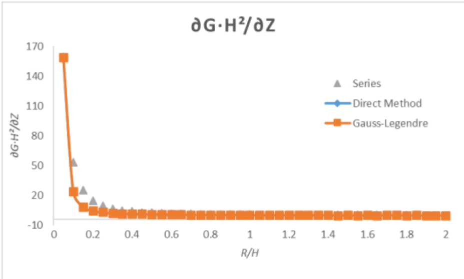

(c) $\frac{\partial G}{\partial z} \cdot h^2$

Fig. **7** The Green function and its derivatives (kh = 0.46268, $\zeta/h = 0$, z/h = -0.01)

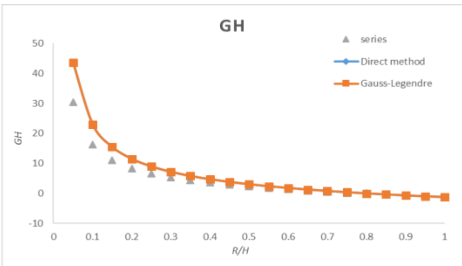

(a) Gh

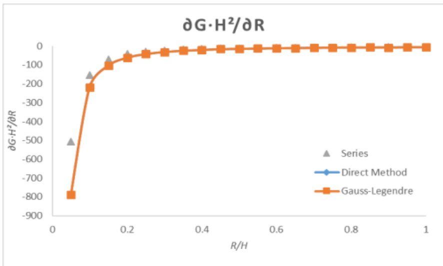

(b) $\frac{\partial G}{\partial R} \cdot h^2$

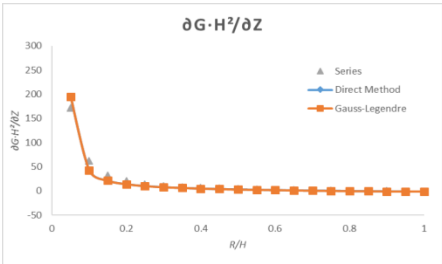

(c) $\frac{\partial G}{\partial z} \cdot h^2$

Fig. 8 The Green function and its derivatives (kh = 1.19968, $\zeta/h = 0$, z/h = -0.01)

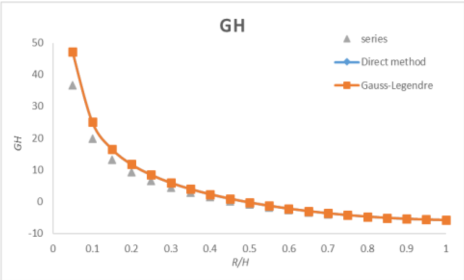

(a) Gh

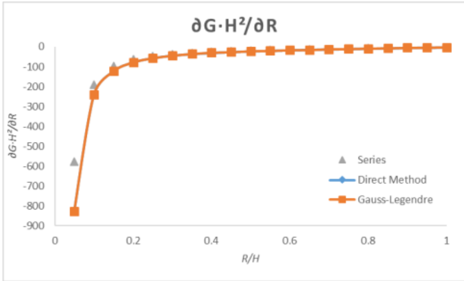

(b) $\frac{\partial G}{\partial R} \cdot h^2$

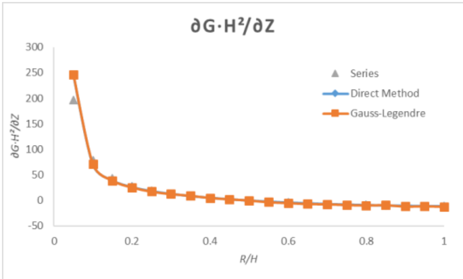

(c) $\frac{\partial G}{\partial z} \cdot h^2$

Fig. 9 The Green function and its derivatives (kh = 2.06534, $\zeta/h = 0$, z/h = -0.01)

Figs. 1-3 present the numerical results of the cases with field points near the water bottom. Since the value of $\partial G/\partial z$ is always 0 when $z/h = -1$, thus $z/h = -0.8$ is chosen to present the numerical results of $\partial G/\partial z$. The numerical results through the Gauss-Legendre integral method show good agreements with the direct calculations using Romberg's method in both the near field and far field, which present an accurate numerical result. The results of the series form have a good coincidence with those from the Gauss-Legendre integral and direct integral calculation with high computational efficiency, but lose precision in the near field when $R/h < 1$.

As there are totally 20 zero points of Legendre polynomial applied to numerically evaluate the Green function and its derivatives in finite water depth, the Gauss-Legendre integral method presents a high computational efficiency in this scenario.

Figs. 7-9 present the numerical results of the cases with field points near the water surface. The numerical results of the Gauss-Legendre integral method agree well with that of direct integral method using Romberg's method in both the near field and far field. As R/h increases, the difference between the results of series form and the other two methods decreases. It should be noted that there are about 100 zero points of the Legendre polynomial applied for the Gauss-Legendre integral method in the water surface case. One reason is that when the field point and source point are both close enough to the water surface, $e^{x(r_2+r_3)}$ mentioned previously converges slowly as x tends to positive infinity. Therefore, there are more Legendre polynomial zero points needed to evaluate the second Gauss-Legendre integral. Through investigation, it can be concluded that less than 20 Legendre polynomial zero points are needed for $r_2 + r_3 \leq -0.2$, 50 points for $-0.2 < r_2 + r_3 \leq -0.05$ and about 100 points are needed for $-0.05 < r_2 + r_3 \leq$

-0 to promise the numerical accuracy. Further investigation is needed in this scenario to evaluate the Green function and its derivatives with field point and source point extremely close to the water surface with a higher computational efficiency. The Gauss-Legendre integral method is practical to evaluate the Green function and its partial derivatives in finite water depth in the near field ($R/h \leq 1$) with a high computational efficiency, combined with series form in the far field ($R/h > 1$).

5. Conclusions

The Green function and its partial derivatives in finite water depth are numerically evaluated in this research to predict the hydrodynamic motion and load response of offshore structures. The Gauss-Legendre integral method is applied to evaluate the integral form of the Green function, whose numerical results are compared with those of other numerical methods.

- The results of the Gauss-Legendre method show a good agreement with the direct integral method in both the near field and far field and series form in the far field.
- The computational efficiency of the case with the field point near the water bottom is higher than that of the case with the field point near the free surface, due to the convergence of the exponential term.
- It is found that the series form presents a high accuracy and computational efficiency in the far field, but loses precision in the near field. Considering the computational efficiency and accuracy.
- It is suggested in this paper to apply the Gauss-Legendre integral method while $R/h \leq 1$ and the series form while $R/h > 1$ to numerically evaluate the Green function and its derivatives in finite water depth.

References

Abramowitz, M. and Stegun, I. A., (1964), *Handbook of Mathematical Functions with Formulas, Graphs, and Mathematical Tables,* Government Printing Office, Washington, and Dover, New York, USA.

Guha, A. and Falzarano, J.M. (2016), "The effect of small forward speed on prediction of wave loads in restricted water depth", *Ocean Syst. Eng*., **6**(4), 305-324.

John, F. (1950), "On the motion of floating bodies, communication of pure applied mathematics", **3**, 45-101.

Li, L. (2001), "Numerical seakeeping predictions of shallow water effect on two ship interactions in waves", PhD. Dissertation, Dalhousie University, Canada.

Liu, R.M., Ren, H.L. and Li, H. (2008), "An improved Gauss-Laguerre method for finite water depth green function and its derivatives", *J. Ship Mech*., **12**(2), 188-196.

Liu, Y. and Falzarano, J. M., (2016), "Suppression of irregular frequency in multi-body problem and free-surface singularity treatment", *Proceedings of the ASME 2016 35th international conference on ocean, offshore and arctic engineering,* Busan, South Korea, June.

Liu, Y.J. and Falzarano, J.M. (2017), "Suppression of Irregular Frequency Effect in Hydrodynamic Problems and Free-Surface Singularity Treatment", *J. Offshore Mech. Arct.* (Accepted)

Liu, Y.J. and Falzarano, J.M. (2017), "A method to remove irregular frequencies and log singularity evaluation in wave-body interaction problems", *J. Ocean Eng. Mar. Energy*. **3**(2), 161-189.

Liu, Y.J. and Falzarano, J.M. (2017), "Irregular frequency removal methods: Theory and applications in hydrodynamics", *J. Mar. Syst. Ocean Technol.*, **12** (2), 49-64.

Liu, Y.J. and Falzarano J.M. (2017) "A note on the conclusion based on the generalized stokes theorem" *J. Offshore Eng. Technol.* (Accepted)

Liu, Y. and Falzarano, J.M. (2017), "Improvement on the accuracy of mean drift force calculation", *Proceedings of the ASME 2017 36th International Conference on Ocean, Offshore and Arctic Engineering*, Trondheim, Norway, June.

Newman, J.N. (1984), "Approximations for the bessel and struve functions", *Math. Comput.*, **43**(168), 551-556.

Newman, J.N. (1985), "Algorithms for the free-surface green function", *J. Eng. Math.*, **19**, 57-67.

Noblesse, F. (1982), "The green function in the theory of radiation and diffraction of regular water waves by a body", *J. Eng. Math.*, **16**, 137-169.

Noblesse, F. (1983), "Integral identities of potential theory of radiation and diffraction of regular water waves by a body", *J. Eng. Math.*, **17**, 1-13.

Telste, J.G. and Noblesse, F. (1986), "Numerical evaluation of the green function of water-wave radiation and diffraction", *J. Ship Res.*, **30** (2), 69-84.

Wang, R.S. (1992), "The numerical approach of three dimensional free-surface green function and its derivatives", *J. Hydrodynamics*, **7**(3), 277-286.

Wehausen, J.V. and Laitone, E.V. (1960), "Surface waves", *Encyclopedia Phys.*, **9**, 446-815.

Wang, H. and Falzarano, J.M. (2017), "Energy balance analysis method in oscillating type wave converter", *J. Ocean Eng. Mar. Energy*, **3**(3), 193-208.

Wu, H., Zhang, C.L., Zhu, Y., Li, W., Wan, D.C. and Noblesse, F. (2017), "A global approximation to the Green function for diffraction radiation", *Eur. J. Mech. B/Fluid.*, **65**, 54-64.

Yu, M. and Falzarano, J.M. (2017), "A comparison of the neuman-kelvin and rankine source methods for wave resistance calculations", Ocean Syst. Eng. (Accepted)

Yang, P., Gu, X.K., Tian, C., Cheng, X.M. and Ding, J. (2014), "Numerical study of 3D pulsating source green function of finite water depth", *Proceedings of the ASME 2014 33rd International Conference on Ocean, Offshore and Arctic Engineering*, San Francisco, USA, June.

MK